

Probing localized states with spectrally resolved speckle techniques

H. Cao, Y. Ling, J. Y. Xu, and A. L. Burin

Department of Physics and Astronomy, Northwestern University, Evanston, Illinois 60208

(Received 26 June 2001; published 23 August 2002)

We have studied the spatial extent of localized states in random media using speckle correlation techniques. Optical gain is introduced to a local region of a random medium to induce lasing of the localized states. The far-field speckle pattern of laser emission from a localized state gives its spatial field correlation function at the surface of the random medium. The envelope of the spatial field correlation function decays exponentially with the transverse coordinate on the surface. The decay length is independent of the pumping rate and the excitation area. We demonstrate that localized states exist in a disordered system that does not reach the localization threshold.

DOI: 10.1103/PhysRevE.66.025601

PACS number(s): 71.55.Jv, 42.30.Ms, 42.25.Fx, 42.25.Dd

Speckle analysis is a powerful tool used to study light transport in disordered media [1–4]. When coherent light is scattered by a disordered medium, the intensity of the emergent wave exhibits an apparently random spatial variation known as speckle. The speckle pattern represents a sample-specific fingerprint that contains detailed information of the random medium. In this work we apply the speckle correlation technique to the study of localized states in a random medium.

The eigenmodes of the Maxwell equations in a disordered dielectric medium can be divided into two categories: extended states and localized states. The wave function of an extended state is spread more or less uniformly throughout the entire medium, while the wave function of a localized state is concentrated in some part of the medium. The dwell time of photons in a localized state is longer than that in an extended state, due to the lower escaping rate of photons through the boundaries. It is unclear whether localized states exist in a three-dimensional random medium far from the localization threshold. Over the past decade, there has been much theoretical study of the anomalously localized states for electrons in the metallic regime [5]. However, there is no direct experimental observation of such states yet. Even if the localized states exist in the diffusion regime, their number is much less than that of the extended states. Thus, the extended states dominate the transport properties. The localized states contribute only to the tail of the time of flight distribution at long delay time. Therefore, it is hard to probe the localized states in the transmission measurement. A new way of probing the localized states is to introduce optical gain to a local region of the random medium [6]. Since the extended states have less spatial overlap with the gain volume than those localized states that occupy the gain volume, the effective gain for the extended states is less. Besides, the localized states have a longer lifetime (lower decay rates) than the extended states. Hence, the localized states lase first as the pumping rate increases. Once the localized states lase, their intensity is much higher than that of the extended states. Thus, they dominate the emission spectrum and the field pattern. The lasing peaks in the spectrum reveal the frequencies of the localized states. The critical pumping rates for lasing reflect the lifetimes of the localized states. Since the wave functions of the localized states may overlap spatially, it is

difficult to tell the spatial extent of each lasing state from the image of the emitted light distribution at the surface of the random medium.

In order to understand the nature of the localized states, it is essential to know their wave functions. Unfortunately, it is impossible to measure the distribution of light field inside the random medium. Nevertheless, information of the wave functions of the localized states at the surface of the random medium gives an important clue. In this paper we use a method named the spectrally resolved speckle analysis to study the spatial profile of individual localized states at the surface of a random medium. We first induce lasing of the localized states with optical pumping, then measure the speckle patterns of coherent emission from individual lasing states. Using Fourier transform, we obtain the spatial field correlation functions of individual localized states at the surface of the random medium. Our work is different from the previous studies of speckle in two respects. (i) We measure the speckle of coherent *emission* from the random medium. (ii) The speckle patterns are *frequency* resolved.

We have measured the localized states in two kinds of random media. One is the polymer containing dye and microparticles. The other is the closely packed semiconductor nanoparticles. In the polymer the dye is the gain medium, and the microparticles are the scattering centers. Because the transport mean free path is much longer than the optical wavelength, the system is far from the localization threshold. In the semiconductor powder, the nanoparticles serve as both the gain medium and the scattering element. The transport mean free path is on the order of the emission wavelength, thus the system is close to the localization threshold. We find localized states exist in both random media but they are very different in size.

The polymer samples are poly(methyl methacrylate) (PMMA) sheets containing rhodamine 640 perchlorate dye and titanium dioxide (TiO₂) microparticles [7]. The thickness is between 0.5 mm and 1 mm. The frequency-doubled output ($\lambda = 532$ nm) of a mode-locked Nd:YAG (yttrium aluminum garnet) laser (10 Hz repetition rate, 30 ps pulse width) is used to excite the dye molecules in the sample. The experimental geometry is shown schematically in Fig. 1(a). The pump beam is focused by a lens of 5 cm focal length onto the polymer sheet at normal incidence. The pump spot at the sample surface is about 50 μm in diameter. The emis-

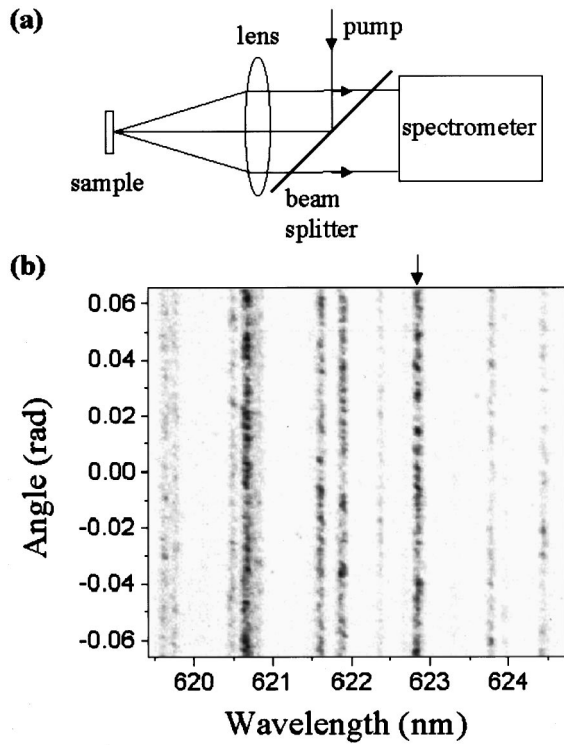


FIG. 1. (a) Schematic experimental geometry for the spectrally resolved speckle measurement of laser emission from the random medium. (b) Part of a spectral image of the emission from the polymer containing dye and microparticles. The incident pump pulse energy is $0.98 \mu\text{J}$.

emission from the sample is collimated by the same lens and directed to a 0.5-m spectrometer with a cooled charge-coupled device (CCD) array detector. The distance from the lens to the spectrometer's entrance slit is equal to the focal length of the lens. Because the polymer sheet is placed at the focal plane of the lens, the emission from the polymer sheet is collimated before entering the spectrometer. When the emission area is very small compared to the focal length of the lens, the emission angle corresponds to the vertical coordinate along the entrance slit of the spectrometer. The spectrometer images its entrance slit onto the two-dimensional (2D) CCD array detector with a 1:1 ratio.

Figure 1(b) shows part of a spectral image above the lasing threshold. The horizontal axis is the wavelength, and the vertical axis is the angle. The dye concentration is 30 mM and Ti_2O particle density is $1.4 \times 10^{12} \text{ cm}^{-3}$. The coherent backscattering measurement of the polymer with the same TiO_2 particle density but no dye gives $kl=32$ [7]. At low pump intensity, the emission spectrum has a single broad spontaneous emission peak. The spontaneous emission intensity is invariant with the angle. When the pump intensity exceeds a threshold, discrete narrow peaks emerge in the emission spectrum. For each spectral peak, the emission intensity fluctuates randomly with the angle. The emergence of speckle is a direct evidence of coherent emission from the sample. As shown in Fig. 1(b), different spectral peaks have different speckle patterns. When the pump intensity increases further, the contrast of the speckle pattern, i.e., the amplitude of intensity variation, increases as the emission becomes more coherent.

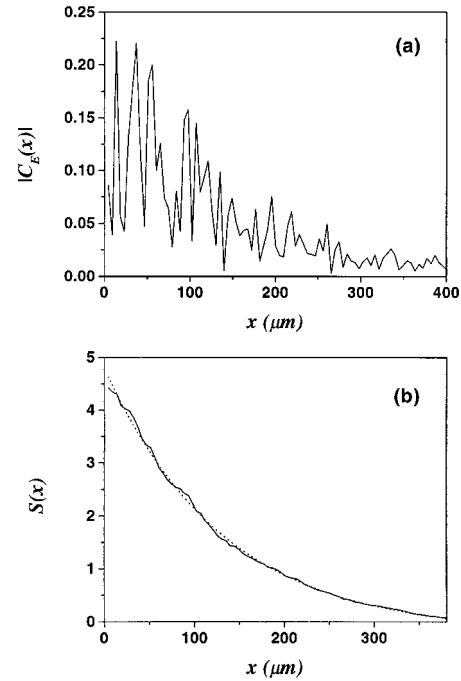


FIG. 2. (a) The amplitude of the spatial field correlation function $|C_E(x)|$ for the lasing peak at $\lambda=622.8 \text{ nm}$ in Fig. 1(b) (marked by an arrow). (b) The solid line is $S(x)$ obtained by integrating $|C_E(x)|$ in (a). The dotted line represents the fit with an exponential decay function.

The far-field speckle pattern of a lasing state is determined by its field pattern at the sample surface. The angular distribution of the outgoing field $E(q)$ is the Fourier transform of the field pattern $E(x)$ at the surface,

$$E(q) = \int E(x) e^{i 2\pi q x} dx, \quad (1)$$

where $q \equiv \sin \theta / \lambda$, θ is the angle between the emission direction and the normal to the sample-air interface, and x represents the transverse coordinate at the sample surface. The angular distribution of the emission intensity $I(q) \equiv |E(q)|^2$ can be obtained experimentally from the far-field speckle pattern. The spatial field correlation function at the sample surface $C_E(x) \equiv \int E^*(x') E(x+x') dx'$. According to Eq. (1), $C_E(x)$ and $I(q)$ form a Fourier transform pair, namely,

$$C_E(x) = \int I(q) e^{-i 2\pi x q} dq. \quad (2)$$

Therefore, the speckle pattern of a lasing state gives its spatial field correlation function.

From the 2D spectral image shown in Fig. 1(b), we obtain the angular dependence $I(q)$ of the emission intensity for the lasing peak at $\lambda=622.8 \text{ nm}$ (marked by an arrow). $I(q)$ is normalized: $\langle I(q) \rangle = 1$. Using discrete Fourier transform, we get the spatial field correlation function, whose amplitude is plotted in Fig. 2(a). The spatial resolution δx for $C_E(x)$ is determined by the angular range Δq of $I(q)$, i.e., $\delta x = 1/\Delta q$. Because the diameter of the lens is larger than the width of the CCD array detector, the maximum collecting angle for the emission $\theta_m = \arctan(D/2f) = 0.066$, where f

$=50$ mm is the focal length of the lens and $D=6.6$ mm is the width of the CCD array detector. Since $\theta_m \ll 1$, $\sin\theta \approx \theta$, and $q \approx \theta/\lambda$. $\Delta q \approx 2\theta_m/\lambda \approx D/f\lambda \approx 0.21 \mu\text{m}^{-1}$. $\delta x \approx 4.7 \mu\text{m}$. The spatial range Δx for $C_E(x)$ is determined by the angular resolution δq , i.e., $\Delta x = 1/\delta q$. Since the emitted light is collimated by the lens, the angular resolution depends on the size s of each CCD pixel. $s = 26 \mu\text{m}$. $\delta q \approx s/f\lambda = 0.832 \text{ mm}^{-1}$. $\Delta x \approx 1.2$ mm. As a result of Fourier transform in the finite range of q , the value of $C_E(0)$ is inaccurate and should be discarded.

As shown in Fig. 2(a), the profile of $|C_E(x)|$ has some peaks and valleys. It reflects the field pattern $E(x)$. We laterally shift the entrance slit of the spectrometer to take a different one-dimensional cut of the two-dimensional speckle pattern. Although $I(x)$ changes completely, the resulting $|C_E(x)|$ is almost the same. The integration of $|C_E(x)|$ gives

$$S(x) \equiv \int_x^\infty |C_E(x')| dx' \approx \int_x^{\Delta x/2} |C_E(x')| dx'. \quad (3)$$

Experimentally $|C_E(x)|$ falls to nearly zero when x approaches $\Delta x/2$. Hence, we replace ∞ by $\Delta x/2$ for the upper limit of the integral in Eq. (3). Figure 2(b) plots $S(x)$ obtained by integrating $|C_E(x)|$ in Fig. 2(a). $S(x)$ is a smoother function of x than $|C_E(x)|$. The dotted line in Fig. 2(b) represents the fit of $S(x)$ with an exponential decay function, $S(x) = A \exp(-x/l_d)$, where A and l_d are the fitting parameters. $S(x)$ fits very well with the exponential decay function, the chi-squared $\chi^2 = 0.0026$. The decay length l_d is $131.8 \mu\text{m}$. We also fit $S(x)$ with an algebraic decay function $S(x) = c_1/x^{c_2}$, where c_1 and c_2 are the fitting parameters. The fit is very bad, $\chi^2 = 0.46$. We repeat the speckle analysis for different lasing peaks in Fig. 1(b). Their spatial field correlation functions are different. Nevertheless, $S(x)$ always fits well with an exponential decay function, but not an algebraic decay function. The decay length varies from peak to peak. The exponential decay of $S(x)$ suggests that the envelope of the spatial field correlation function falls exponentially with x , namely, $|C_E(x)| \sim \exp(-x/l_d)$.

We have measured the spatial field correlation functions over a wide range of pump intensity, from the threshold where discrete spectral peaks appear to well above the threshold. Figure 3(a) plots the decay length l_d versus the pump intensity for a particular lasing state. The pump intensity I_p is normalized to the threshold value I_0 where this lasing peak just emerges in the emission spectrum. We fit $S(x)$ with an exponential decay function. The fitting error χ^2 is shown in Fig. 3(b). Just above the threshold, the exponential fit of $S(x)$ is not good, as indicated by the relatively large value of χ^2 . The decay length $l_d = 365 \mu\text{m}$. With an increase of the pump intensity, χ^2 decreases, suggesting that the exponential fit becomes better. The decay length also decreases. Eventually, $S(x)$ fits very well with an exponential decay. The decay length does not change with the pump intensity any more. The behavior of the decay length can be explained as follows. When the lasing peak just appears in the emission spectrum, its intensity is lower than the amplified spontaneous emission intensity. The large decay length indicates the amplified spontaneous emission is spread over a

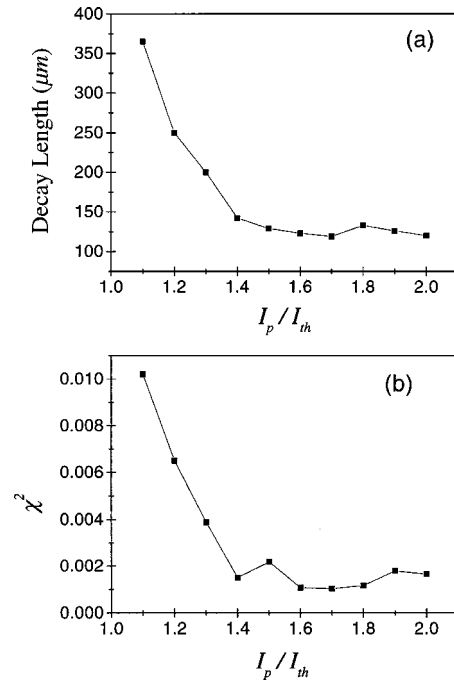


FIG. 3. (a) The decay length as a function the pump intensity I_p normalized to the threshold value I_0 . (b) The fitting error χ^2 versus the normalized pump intensity I_p/I_0 .

large region. As the pump intensity increases, the emission intensity of the lasing state increases more rapidly than the amplified spontaneous emission intensity. When the emission intensity of the lasing state becomes much higher than the amplified spontaneous emission intensity, the wave function of the lasing state dominates the spatial field correlation function. The independence of the decay length on the pump intensity suggests the wave function of the lasing state does not change with the pumping rate. This conclusion agrees with the result of theoretical modeling [6,8].

The decay length of a lasing state is also independent of the excitation area. We vary the diameter of the pump spot at the sample surface from 50 to $400 \mu\text{m}$ by adding two lens and an aperture to the optical path of the pump beam. When the pump power is fixed and the excitation area is reduced, some states with longer decay length stop lasing, while some states with shorter decay length start lasing. This is because the smaller states have more spatial overlap with the gain volume when the diameter of the pump spot is smaller than the decay length. The effective gain for the smaller states is higher, thus it is easier for them to lase. However, some states keep lasing as the pump area is varied. Their decay lengths do not change with the pump area.

For comparison, we focus a He:Ne laser beam onto our sample and measure the speckle of the scattered laser light. In the absence of optical pumping, the polymer sheet is a passive random medium. The experimental setup is shown in the inset of Fig. 4. To keep the reflected beam away from the entrance slit of the spectrometer, the incident angle of the He:Ne laser beam is set at $\sim 45^\circ$. The diameter of the incident beam spot at the sample surface is $\sim 80 \mu\text{m}$. From the far-field speckle pattern, we get $I(q)$, and normalize it $\langle I(q) \rangle = 1$. Fourier transform of $I(q)$ gives $C_E(x)$. Figure 4 plots $S(x)$. The dotted line represents an exponential fit of

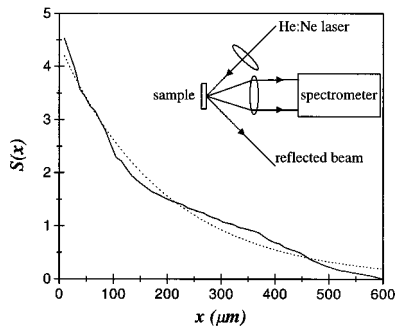


FIG. 4. The solid line represents $S(x)$, obtained by integrating $C_E(x)$ for the scattered He:Ne laser light. The dashed line represents the fit with an exponential decay function. The inset is a schematic diagram of the experimental setup.

$S(x)$. The fit is quite bad, $\chi^2=0.025$. We shift the sample so that the laser beam hits different part of the sample, and we repeat the speckle measurement. Similar results are obtained. Neither $S(x)$ nor its ensemble average fit an exponential decay function.

The spatial field correlation function $C_E(x)$ at the surface of a passive random medium has been derived from the diffusion theory [9]. In the calculation, a coherent light transmits through a thick slab. The light intensity at the exit face is assumed constant. The envelope of $|C_E(x)|$ is inversely proportional to the transverse coordinate x on the surface, as is confirmed experimentally in a quasi-one-dimensional system [10]. This dependence is caused by the phase correlation of the field. In our experiment, the incident He:Ne laser beam has a Gaussian profile. Thus, the scattered light intensity varies across the sample surface. The spatial field correlation function is determined not only by the phase correlation, but also by the spatial variation of the field amplitude. The overall profile of $C_E(x)$ at the sample surface depends on the incident beam diameter and the sample absorption. It does not exhibit a simple exponential decay.

Different from the speckle of an external laser light scattered by a passive random medium, the speckle of laser emission from an active random medium gives the spatial field correlation functions of the lasing states. In contrast to that of the scattered He:Ne laser light, the spatial field correlation function of a lasing state does not depend on the excitation area or the pumping rate. Recent theoretical modeling shows that when an eigenstate of a random medium lases, the spatial distribution of laser light field is identical to the wave function of the eigenstate in the passive medium [6,8]. Therefore, the measured spatial field correlation func-

tion of laser emission is determined by the wave function of the state that lases. For a coherent lasing state, the spatial extend of $C_E(x)$ directly reflects the spatial extend of the wave function $E(x)$. Since the lasing state is extended over a region whose size is much smaller than the sample size, it is a localized state. Our measurement result of the polymer samples demonstrates that localized states exist in the disordered system with $kl \gg 1$. Such states may be the optical analog to the anomalously localized states of electrons in the metallic regime [5].

We have also measured the localized states in closely packed ZnO and GaN nanoparticles, where kl is less than 10 but still larger than 1 [11]. The pump light is switched to the third harmonics ($\lambda = 355$ nm) of the pulsed Nd:YAG laser. To increase the range of the collecting angle for emission, we replace the lens with a $20\times$ microscope objective. The focal length of the objective $f = 8.3$ mm. Its diameter is 6.6 mm, equal to the width of the CCD array detector. The angular range $\Delta q = 2.0 \mu\text{m}^{-1}$ and the spatial resolution $\delta x = 0.5 \mu\text{m}$. The angular resolution $\delta q = 8.2 \text{mm}^{-1}$, and the spatial range $\Delta x = 121 \mu\text{m}$. We obtain the spatial field correlation functions of individual lasing states from the Fourier transform of their speckle patterns above the lasing threshold. For all the lasing states, $S(x)$ fits well with the exponential decay function. The decay length varies from $\sim 1.5 \mu\text{m}$ to $\sim 4.0 \mu\text{m}$ for different states. Comparing the localized states in the semiconductor powder to those in the polymer, we find the size of the localized states decreases as the disordered system moves toward the localization threshold.

In summary, the spectrally resolved speckle analysis of laser emission from a random medium gives the spatial field correlation functions for individual lasing states. The envelope of the spatial field correlation function decays exponentially with the transverse coordinate at the sample surface. The decay length varies from state to state, but it is independent of the pumping rate and the excitation area. For a coherent lasing state, the spatial field correlation function directly reflects the wave function. We demonstrate that localized states exist in a random medium far from the localization threshold. With decrease of the transport mean free path, the localized states shrink in size. The introduction of optical gain to a local region of a random medium allows the direct observation of these localized states that are hardly accessible in the transport experiment.

We thank Professor A. Z. Genack for stimulating discussions. This work was partially supported by the National Science Foundation under Grant No. DMR-0093949. H.C. acknowledges support from the David and Lucile Packard Foundation and the Alfred P. Sloan Foundation.

- [1] B. Shapiro, Phys. Rev. Lett. **57**, 2168 (1986).
 [2] M. Kaveh *et al.*, Nature (London) **326**, 778 (1987).
 [3] N. Garcia and A.Z. Genack, Phys. Rev. Lett. **63**, 1678 (1989).
 [4] M. Stoytchev and A.Z. Genack, Opt. Lett. **24**, 262 (1999).
 [5] B. L. Altshuler, V. E. Kravtsov, and I. V. Lerner, in *Mesoscopic Phenomena in Solids* (North-Holland, Amsterdam, 1991).
 [6] C. Vanneste *et al.*, Phys. Rev. Lett. **87**, 183903 (2001).

- [7] Y. Ling *et al.*, Phys. Rev. A **64**, 063808 (2001).
 [8] X. Jiang and C. Soukoulis, Phys. Rev. E **65**, 025601(R) (2002).
 [9] I. Freund and D. Eliyahu, Phys. Rev. A **45**, 6133 (1992).
 [10] P. Sebbah *et al.*, Phys. Rev. E **62**, 7348 (2000).
 [11] H. Cao *et al.*, Phys. Rev. Lett. **82**, 2278 (1999); H. Cao *et al.*, *ibid.* **84**, 5584 (2000).